

# Conversion of a Disulfide Bond into a Thioacetal Group during Echinomycin Biosynthesis\*\*

Kinya Hotta, Ronan M. Keegan, Soumya Ranganathan, Minyi Fang, Jaclyn Bibby, Martyn D. Winn, Michio Sato, Mingzhu Lian, Kenji Watanabe, Daniel J. Rigden, and Chu-Young Kim\*

**Abstract:** Echinomycin is a nonribosomal depsipeptide natural product with a range of interesting bioactivities that make it an important target for drug discovery and development. It contains a thioacetal bridge, a unique chemical motif derived from the disulfide bond of its precursor antibiotic triostin A by the action of an *S*-adenosyl-L-methionine-dependent methyltransferase, Ecm18. The crystal structure of Ecm18 in complex with its reaction products *S*-adenosyl-L-homocysteine and echinomycin was determined at 1.50 Å resolution. Phasing was achieved using a new molecular replacement package called AMPLE, which automatically derives search models from structure predictions based on *ab initio* protein modeling. Structural analysis indicates that a combination of proximity effects, medium effects, and catalysis by strain drives the unique transformation of the disulfide bond into the thioacetal linkage.

Echinomycin **1** is a member of the quinoxaline family of nonribosomal peptide natural products. Quinoxaline antibiotics are characterized by a pair of bicyclic aromatic quinoxaline or quinoline chromophores that are attached to a C<sub>2</sub>-symmetric cyclic depsipeptide core (Figure 1).<sup>[1]</sup> Virtually all members of this family are potent antibiotics against Gram-positive bacteria, as they inhibit DNA-directed RNA synthesis,<sup>[2–5]</sup> and many, including **1** and BE-22179, also possess potent cytotoxic activity against a variety of cultured tumor cells.<sup>[6,7]</sup> Recently, **1** was found to be an inhibitor of

a hypoxia-inducing factor that plays a role not only in controlling cancer cell growth, but also in regulating ovulation<sup>[8]</sup> and the development of pluripotent embryonic stem cells.<sup>[9]</sup> This multitude of biological activities makes the quinoxaline family of nonribosomal peptides interesting targets for drug discovery and development.

Triostin A (**2**) has a cyclic octapeptide core that contains an intra-peptide disulfide bridge. **1** has the same core structure as **2**, but contains a thioacetal bridge in place of the disulfide bridge. This subtle but important structural variation affects the chemical stability and biological activity of these compounds. Both **1** and **2** can intercalate duplex DNA, thereby interfering with its transcription, replication, and repair.<sup>[10]</sup> However, **1** and **2** have distinct DNA-sequence preferences that arise from the structural perturbation that is due to the conversion of the disulfide bridge in **2** into a thioacetal bridge in **1**.<sup>[10]</sup> This structural alteration, which provides higher stability to the bicyclic core in **1** by transforming the labile disulfide bond into a more stable thioacetal linkage, is also thought to contribute to making **1** a more potent anti-tumor agent than **2**.<sup>[11]</sup> However, the chemistry of the transformation of a disulfide bond into a thioacetal linkage is currently not known. To fill this knowledge gap, we set out to elucidate the catalytic mechanism of Ecm18, the enzyme that is responsible for the conversion of disulfide into thioacetal linkages in *Streptomyces lasaliensis*.<sup>[12]</sup> Herein, we present the crystal structure of Ecm18 in complex with its

[\*] Dr. K. Hotta,<sup>[†]</sup> S. Ranganathan, M. Fang, M. Lian, Prof. Dr. C.-Y. Kim  
Department of Biological Sciences  
National University of Singapore  
14 Science Drive 4, Singapore 117543 (Singapore)  
E-mail: chuyoung@nus.edu.sg

Dr. R. M. Keegan  
Research Complex at Harwell  
STFC Rutherford Appleton Laboratory  
Harwell, Oxfordshire (UK)

Dr. J. Bibby, Dr. D. J. Rigden  
Institute of Integrative Biology, University of Liverpool  
Crown Street, Liverpool (UK)

Dr. J. Bibby  
Department of Chemistry, University of Liverpool  
Liverpool (UK)

Dr. M. D. Winn  
Science and Technology Facilities Council, Daresbury Laboratory  
Daresbury (UK)

Dr. M. Sato, Prof. Dr. K. Watanabe  
Department of Pharmaceutical Sciences, University of Shizuoka  
Shizuoka 422-8526 (Japan)

[†] Current address: School of Biosciences  
The University of Nottingham  
Malaysia Campus, Selangor 43500 (Malaysia)

[\*\*] This work was supported by a National University of Singapore–Japan Society for the Promotion of Science Joint Research Project grant (C.-Y.K.), the Biotechnology and Biological Science Research Council (BB/H01330X/1; D.J.R. and M.W.), the 2011 CCP4/OIST School in Protein Crystallography, and the Japan Society for the Promotion of Science (LS103; K.W.). Use of the Advanced Photon Source was supported by the U.S. Department of Energy, Office of Science, Office of Basic Energy Sciences (DE-AC02-06CH11357). Use of the IMCA-CAT beamline 17-ID at the Advanced Photon Source was supported by the companies of the Industrial Macromolecular Crystallography Association through a contract with the Hauptman–Woodward Medical Research Institute. We would like to thank Dr. Andrey Lebedev of the CCP4 group for his expert advice on ligand building and structure solution. The computational infrastructure used by AMPLE in this work was provided by the Research Complex at Harwell and CCP4.



Supporting information for this article is available on the WWW under <http://dx.doi.org/10.1002/anie.201307404>.

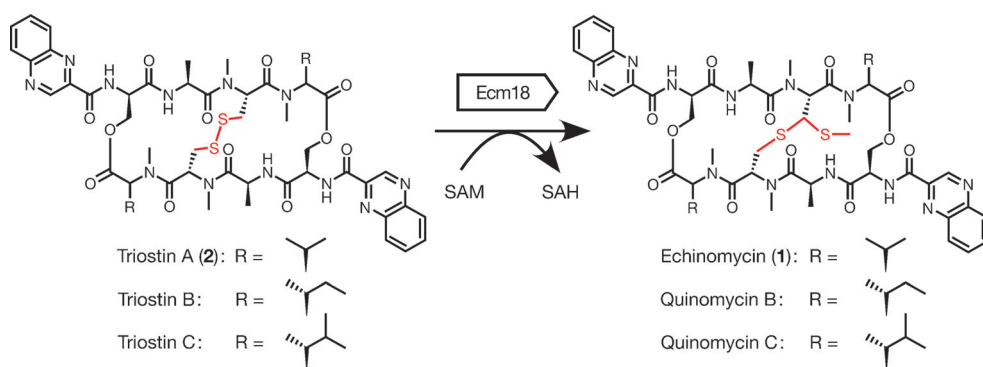


**Figure 1.** Transformation of triostin A (2) into echinomycin (1) by Ecm18, a SAM-dependent methyltransferase. The disulfide bond in 2 and the thioacetal bridge in 1 are highlighted in red. Naturally occurring analogues of 2 and 1 are also shown.

native products echinomycin and *S*-adenosyl-L-homocysteine (PDB ID code: 4NEC) at 1.5 Å resolution, and we propose a catalytic mechanism for the transformation of the disulfide bond into a thioacetal linkage. The crystal structure was determined by molecular replacement performed with the program AMPLER.<sup>[13]</sup> Initially conceived for application to pure ab initio models, it was employed here to derive successful ensemble search models from structure predictions that were informed by the availability of partial and only distantly homologous structures (see the Supporting Information).

The overall fold of Ecm18 is characteristic of the SAM-MTase family of proteins (Figure 2; SAM = *S*-adenosyl-L-methionine, MTase = methyltransferase).<sup>[14]</sup> Specifically, Ecm18 assumes the Class I SAM-MTase fold that is common for MTases that act on DNA and small molecules. Ecm18 is comprised of two domains: a SAM-binding domain and a substrate-binding domain. The SAM-binding domain is

formed mainly by the N-terminal half of the protein, whereas the substrate-binding domain is comprised of the C-terminal half of the molecule and a small N-terminal segment. SAH is bound to the SAM-binding domain of Ecm18 in a conformation similar to that observed in many other SAM-MTase structures, where the central ribose moiety is buttressed against the loop that connects the  $\beta$ 1 strand and the  $\alpha$ A helix that carries the signature GxGxG nucleotide-binding motif (Figure 3; G = glycine, x = any canonical amino acid).<sup>[16]</sup> The cofactor engages in an extensive hydrogen-bonding interaction with the protein and the bound water molecules. On the other hand, the substrate-binding domain of Ecm 18 is formed by  $\alpha$ Y and  $\alpha$ 2 helices,  $3_{10}$

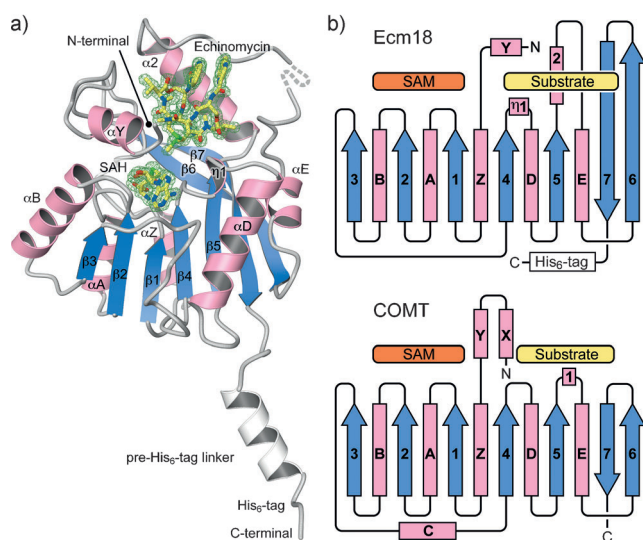


**Figure 2.** a) Overall fold of Ecm18. *S*-Adenosyl-L-homocysteine (SAH) and 1 are shown in stick representation, and their electron densities are shown as green mesh (simulated annealing omit map contoured at 2.0  $\sigma$ ). b) Topology diagram of Ecm18 and the rat catechol-O-MTase (COMT),<sup>[15]</sup> an archetypal class I SAM-dependent methyltransferase.

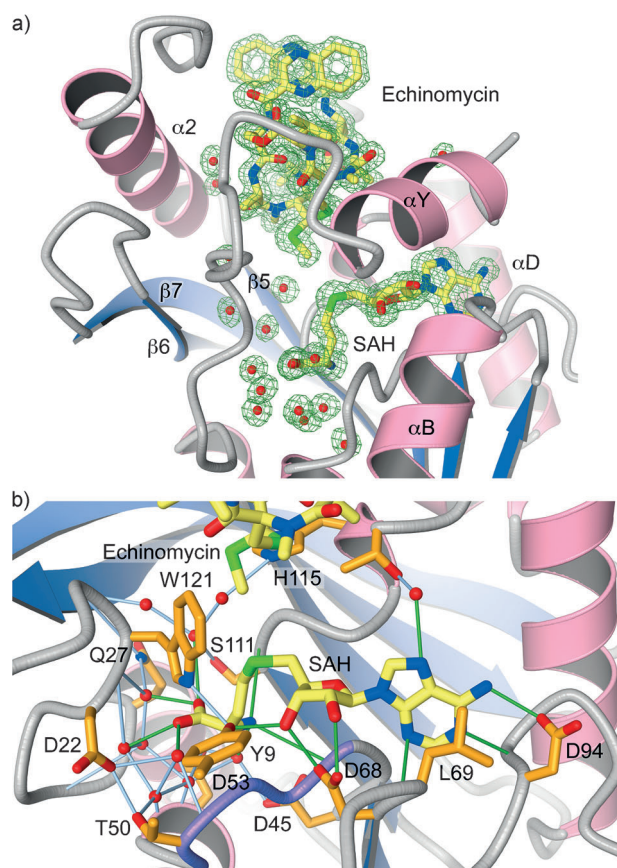


**Figure 3.** Crystal structure of Ecm 18 in complex with echinomycin and SAH. a) Simulated annealing omit map of the bound ligands and water molecules contoured at 1.2  $\sigma$ . Water molecules are represented by red spheres. b) Details of the SAH-Ecm18 interactions; hydrogen bonds between SAH and Ecm18 (—) and secondary-shell hydrogen bonds (—) are shown. The conserved signature GxGxG nucleotide binding motif is highlighted in purple.

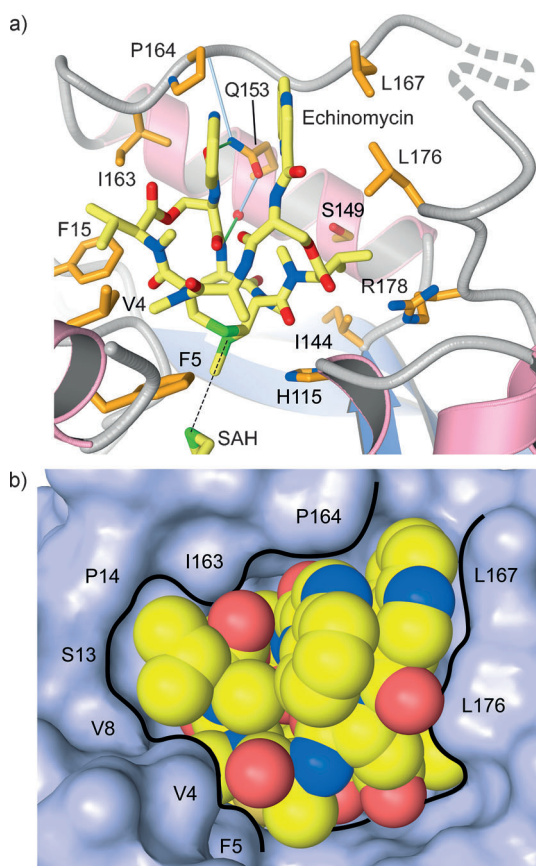


**Figure 4.** Details of the Ecm18–echinomycin interaction. a) Close-up picture of the 1–Ecm18 interaction. The linear arrangement of the SAH sulfur atom, the methyl group that is transferred, and the receiving sulfur atom of 1 is shown (-----). b) Solvent-accessible surface of Ecm18, with bound 1 represented by a space-filling model; the exquisite shape complementarity between the protein binding pocket and the ligand is shown.

helix  $\eta$ 1, the loop that connects  $\alpha$ 2 to  $\alpha$ E, and the extended portion of the  $\beta$ 6 and  $\beta$ 7 strands (Figure 2). Surprisingly, 1 forms only one direct hydrogen bond (involving the carbonyl oxygen of the quinoxaline-2-carboxamide moiety of 1) and one water-mediated hydrogen bond (involving an

Ala residue of 1), both with Gln153 of Ecm18 (Figure 4a). This suggests that the substrate-binding specificity of Ecm18 is driven primarily by shape complementarity (Figure 4b).

The most striking structural feature of the complex between Ecm18 and 1 is the conformation that 1 assumes within the substrate-binding pocket of Ecm18. When bound to Ecm18 (Figure 5a), the peptide core of 1 assumes a conformation that is more compact than those observed in the crystal structures of free 1<sup>[17]</sup> (Figure 5b) or for a complex of 1 with duplex DNA<sup>[18]</sup> (Figure 5c). Consequently, the two quinoxaline moieties in 1 are brought much closer together. The collapsed conformation of 1 in Ecm18 appears to be stabilized by the snug fit between 1 and the Ecm18 binding pocket and through favorable  $\pi$ - $\pi$  interactions between the stacked heteroaromatic rings of the quinoxaline moieties. The native substrate of Ecm18, 2, will also have to have its peptide backbone compactly folded to bind to the active site of Ecm18. However, the structures of 2 that were determined by X-ray crystallography and NMR spectroscopy indicate that 2 assumes an extended conformation when it is free of binding partners<sup>[17,19]</sup> (Figure 5d) or when it is in complex with DNA<sup>[20]</sup> (Figure 5e). In fact, free 2 exhibits a more extended conformation than free 1 (Figure 5d vs. 5b). Thus, 2 will have to undergo a significant restructuring to assume the highly compressed structure that is required for binding to Ecm18. The current crystal structure indicates that the compact folding of 1 involves a *trans*-to-*cis* isomerization of the Ala–MeCys peptide bonds.<sup>[21]</sup> Whereas N-alkylated amide bonds are known to assume a *cis* configuration more readily than a standard peptide bond,<sup>[22]</sup> *cis*-configured peptide bonds in the backbone of 2 are still a disfavored structural element. This observation is in agreement with the occurrence of only a small proportion of *cis*-configured peptide bonds in the ensemble of solution conformers of 2.<sup>[21]</sup> Similarly, only *all-trans* structures were observed by X-ray crystallography and NMR spectroscopy of 2 and 1 (Figure 5b–e). Thus, the requirement for the substrate to assume a highly compact structure with *cis*-configured backbone peptide bonds upon binding to the Ecm18 active site is expected to introduce strain into the bound substrate molecule. The implications of this strain will be discussed later.

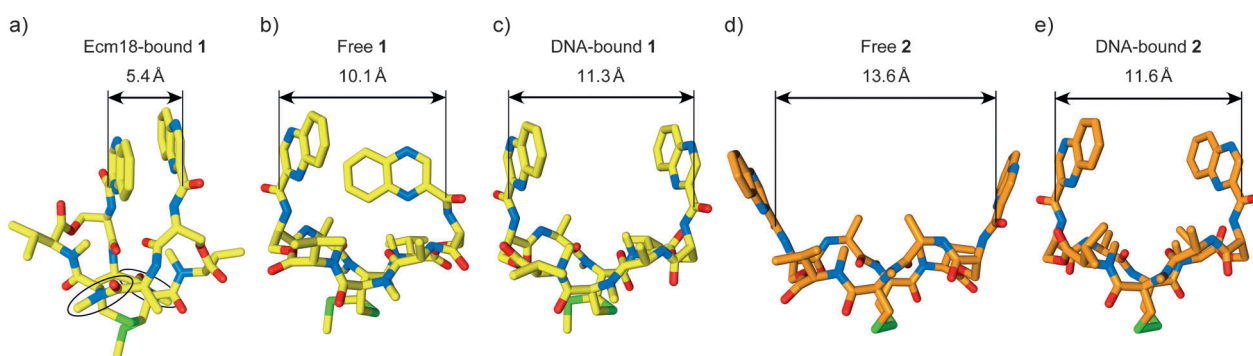


**Figure 5.** Comparison of conformations that 1 (a,b,c) and 2 (d,e) assume under different conditions. The distance between the pair of carbonyl carbon atoms of the quinoxaline-2-carboxamide moieties is given. a) Crystal structure of 1 in complex with Ecm18. The pair of *cis*-peptide bonds present only in the Ecm18-bound 1 is circled. Carbon yellow (1) or orange (2), nitrogen blue, oxygen red, sulfur green. b) Crystal structure of 1 in the absence of any binding partner.<sup>[17]</sup> c) Crystal structure of 1 in complex with DNA.<sup>[18]</sup> d) Crystal structure of 2 in the absence of any binding partner.<sup>[17]</sup> e) Structure of 2 in complex with DNA determined by NMR spectroscopy.<sup>[20]</sup>



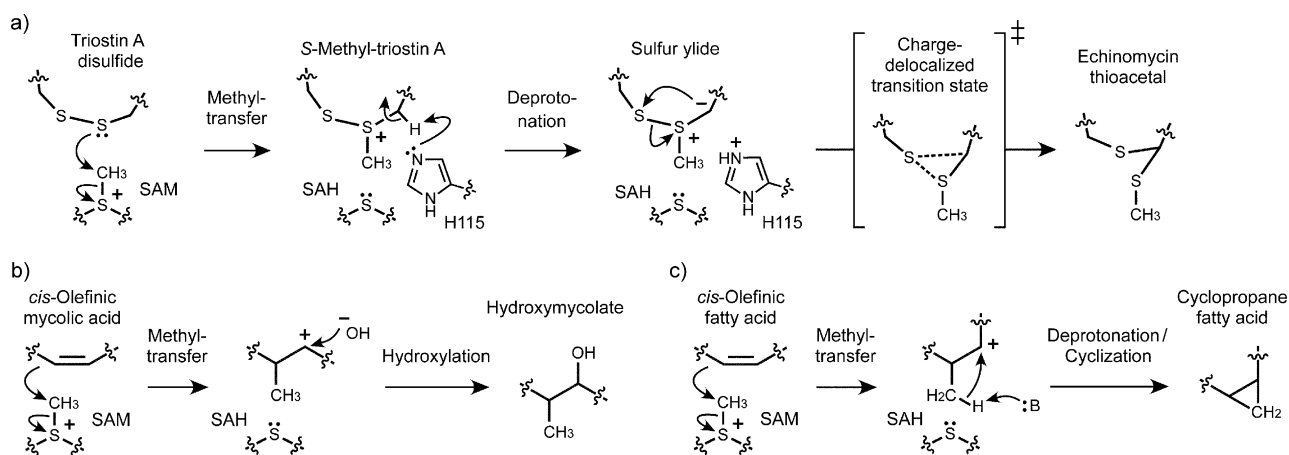


**Figure 6.** Mechanism of methylation-initiated modification of different metabolites. a) Proposed conversion of the disulfide bond in **2** into the thioacetal bridge in **1**. b) Methylation/hydroxylation of an olefin during the biosynthesis of hydroxymycolate.<sup>[23]</sup> c) Methylation-initiated cyclopropane formation during the biosynthesis of *Escherichia coli* *cis*-cyclopropane fatty acid.<sup>[24]</sup>

The conversion of **2** into **1** by Ecm 18 can be divided into two stages. The initial stage involves methylation of one of the sulfur atoms from the disulfide bond of **2** (Figure 6a). In the second stage, the methylated disulfide bond undergoes a rearrangement to form the thioacetal bridge of **1**. Previous studies have established that methyl transfer reactions that are catalyzed by SAM-MTases proceed through an  $S_N2$ -type nucleophilic attack on the methyl group of SAM by the nucleophile.<sup>[25]</sup> The structure that was obtained for Ecm18 supports this hypothesis in that the methionyl sulfur atom of SAH, the transferred methyl group, and the nucleophilic sulfur atom of **1** are present in a linear arrangement (Figure 4a; .....). The only residue in the vicinity of the disulfide bond that could act as a catalytic base is His115. However, unlike in most other SAM-MTases where the nucleophile is a carbon, nitrogen, or oxygen atom that may require activation through deprotonation, the nucleophile in the Ecm18-catalyzed methyl transfer reaction is an electron-rich sulfur atom of a disulfide bond. Thus, activation of the sulfur atom as a nucleophile is perhaps not required for the methyl transfer reaction to proceed. Instead, the Ecm18-catalyzed methyl transfer reaction is likely to be driven by the proximity effect; the enzyme enables the transformation by bringing the sulfur atom of the substrate close to the activated methyl group of the cofactor in a favorable orientation. When Ecm 18 is provided with the open form of **2**, in which the disulfide bridge has been reduced, the reaction halts after the methylation step (Supporting Information, Figure S1). The trapping of this mono-methylated product provides biochemical support for the proposed two-stage reaction mechanism.

The second stage of the Ecm18-catalyzed transformation is the rearrangement of the methylated disulfide bond of **2** into the thioacetal bridge of **1** (Figure 6a). This rearrangement can be initiated by the abstraction of a proton from the carbon atom adjacent to the tertiary sulfonium cation, which leads to the formation of a sulfur ylide intermediate. This deprotonation is likely to be the primary function of His115, whose N $\epsilon$ 2 atom of the imidazole group is 3.7 Å away from the target carbon atom in the Ecm18-product complex. The

occurrence of a charged sulfonium species within the relatively hydrophobic microenvironment of the Ecm18 binding pocket, which is also shielded from the bulk solvent by the bound substrate itself, can cause a significant lowering of the  $pK_a$  value of the proton to be abstracted,<sup>[26]</sup> which renders proton abstraction by the imidazole group of His115 feasible. Once the sulfur ylide is formed, the carbanion of the ylide can attack the neutral sulfur atom adjacent to the ylide sulfonium to complete the rearrangement through the formation of a three-membered ring transition state to yield a neutral thioacetal linkage. Again, a general lack of charged or polar side chains in the vicinity of the sulfur ylide appears to play an important role in accelerating the reaction.

When the overall conversion of **2** into **1** is considered, the formation of the Ecm18-**2** complex may incur greater binding energy expenditure than the energy contained in the final Ecm18-**1** complex because folding the peptide backbone of **2** into a *cis* configuration is presumably more difficult, because free **2** assumes a more extended conformation than free **1** (Figure 5d vs. 5b).<sup>[17]</sup> Furthermore, the rigid and shorter thioacetal bridge of **1** may be favored over the more flexible and longer disulfide bond of **2** within the Ecm18 binding pocket where the bound ligand is required to be compact. Thus, the transformation of the disulfide bond into a thioacetal linkage, which concurrently releases strain in the bound substrate, may play an important role in driving the reaction forward. Taken together, proximity effects, medium effects, and catalysis by strain appear to work in synergy to render Ecm18 an effective catalyst for the transformation of the disulfide bond into a thioacetal linkage during echinomycin biosynthesis.

There are other methyltransferases that use methylation as an initial step for catalyzing the formation of chemical structures that are beyond simple methylated products. For example, mycolic acid MTase initially catalyzes a methylation of one carbon atom of an olefin of a fatty acid prior to hydroxylating the other carbon atom to generate oxygenated mycolic acids (Figure 6b).<sup>[23]</sup> Similarly, cyclopropane fatty acid synthase also uses an initial SAM-dependent methylation

to promote the formation of a cyclopropane moiety during the biosynthesis of cyclopropane fatty acid (Figure 6c). In the latter case, methylation of an olefin leads to the formation of a carbocation that is subsequently attacked by a base-activated methyl group to yield a cyclopropane moiety.<sup>[24]</sup> The Ecm18-catalyzed process represents a new and unique addition to the list of transformations that SAM-MTases can accomplish.

Received: August 22, 2013

Revised: October 1, 2013

Published online: December 2, 2013

**Keywords:** biosynthesis · disulfides · peptides · transferases · thioacetals

- [1] D. L. Boger, S. Ichikawa, W. C. Tse, M. P. Hedrick, Q. Jin, *J. Am. Chem. Soc.* **2001**, *123*, 561–568.
- [2] F. Romero, F. Espliego, J. Pérez Baz, T. García de Quesada, F. de La Calle, J. L. Fernández-Puentes, *J. Antibiot.* **1997**, *50*, 734–737.
- [3] M. Waring, A. Makoff, *Mol. Pharmacol.* **1974**, *10*, 214–224.
- [4] F. Takusagawa, *J. Antibiot.* **1985**, *38*, 1596–1604.
- [5] S. Toda, K. Sugawara, Y. Nishiyama, M. Ohbayashi, N. Ohkusa, H. Yamamoto, M. Konishi, T. Oki, *J. Antibiot.* **1990**, *43*, 796–808.
- [6] B. J. Foster, K. Clagett-Carr, D. D. Shoemaker, M. Suffness, J. Plowman, L. A. Trissel, C. K. Grieshaber, B. Leyland-Jones, *Invest. New Drugs* **1985**, *3*, 403–410.
- [7] H. Okada, H. Suzuki, T. Yoshinari, H. Arakawa, A. Okura, H. Suda, A. Yamada, D. Uemura, *J. Antibiot.* **1994**, *47*, 129–135.
- [8] J. Kim, I. C. Bagchi, M. K. Bagchi, *Endocrinology* **2009**, *150*, 3392–3400.
- [9] S. N. Greer, J. L. Metcalf, Y. Wang, M. Ohh, *EMBO J.* **2012**, *31*, 2448–2460.
- [10] J. S. Lee, M. J. Waring, *Biochem. J.* **1978**, *173*, 115–128.
- [11] K. R. Fox, M. J. Waring, *Biochim. Biophys. Acta Nucleic Acids Protein Synth.* **1981**, *654*, 279–286.
- [12] K. Watanabe, K. Hotta, A. P. Praseuth, K. Koketsu, A. Migita, C. N. Boddy, C. C. Wang, H. Oguri, H. Oikawa, *Nat. Chem. Biol.* **2006**, *2*, 423–428.
- [13] J. Bibby, R. M. Keegan, O. Mayans, M. D. Winn, D. J. Rigden, *Acta Crystallogr. Sect. D* **2012**, *68*, 1622–1631.
- [14] H. L. Schubert, R. M. Blumenthal, X. Cheng, *Trends Biochem. Sci.* **2003**, *28*, 329–335.
- [15] J. Vidgren, L. A. Svensson, A. Liljas, *Nature* **1994**, *368*, 354–358.
- [16] P. Z. Kozbial, A. R. Mushegian, *BMC Struct. Biol.* **2005**, *5*, 19.
- [17] G. M. Sheldrick, A. Heine, K. Schmidt-Bäse, E. Pohl, P. G. Jones, E. Paulus, M. J. Waring, *Acta Crystallogr. Sect. B* **1995**, *51*, 987–999.
- [18] R. Pföh, J. A. Cuesta-Seijo, G. M. Sheldrick, *Acta Crystallogr. Sect. F* **2009**, *65*, 660–664.
- [19] Y. Kyogoku, N. Higuchi, M. Watanabe, K. Kawano, *Biopolymers* **1981**, *20*, 1959–1970.
- [20] K. J. Address, J. Feigon, *Biochemistry* **1994**, *33*, 12386–12396.
- [21] T. V. Alfredson, A. H. Maki, M. J. Waring, *Biopolymers* **1991**, *31*, 1689–1708.
- [22] K. Nguyen, M. Iskandar, D. L. Rabenstein, *J. Phys. Chem. B* **2010**, *114*, 3387–3392.
- [23] F. Boissier, F. Bardou, V. Guillet, S. Uttenweiler-Joseph, M. Daffé, A. Quémard, L. Mourey, *J. Biol. Chem.* **2006**, *281*, 4434–4445.
- [24] D. F. Iwig, A. Uchida, J. A. Stromberg, S. J. Booker, *J. Am. Chem. Soc.* **2005**, *127*, 11612–11613.
- [25] R. W. Woodard, M. D. Tsai, H. G. Floss, P. A. Crooks, J. K. Coward, *J. Biol. Chem.* **1980**, *255*, 9124–9127.
- [26] F. Jordan, H. Li, A. Brown, *Biochemistry* **1999**, *38*, 6369–6373.